

Supplementary Information

Dynamic interactome of the MHC I peptide loading complex in human dendritic cells

Martina Barends^{1,#}, Nicole Koller^{1,#}, Christian Schölz^{2,†}, Verónica Durán^{3,§}, Berislav Bošnjak⁴,
Jennifer Becker³, Marius Döring³, Hanna Blee¹, Reinhold Förster^{4,5}, Ulrich Kalinke^{3,5},
Robert Tampé^{1,*}

¹Institute of Biochemistry, Biocenter, Goethe University Frankfurt, Max-von-Laue-Str. 9,
60438 Frankfurt am Main, Germany

²Max von Pettenkofer Institute and Gene Center, Virology, National Reference Center for
Retroviruses, Faculty of Medicine, Ludwig-Maximilians-Universität München, Pettenkoferstraße
9a, 80336 Munich, Germany

³Institute for Experimental Infection Research, TWINCORE, Centre for Experimental and Clinical
Infection Research, a Joint Venture between the Helmholtz Centre for Infection Research and the
Hannover Medical School, 30625 Hannover, Germany

⁴Institute of Immunology, Hannover Medical School, Carl-Neuberg-Str. 1,
30625 Hannover, Germany

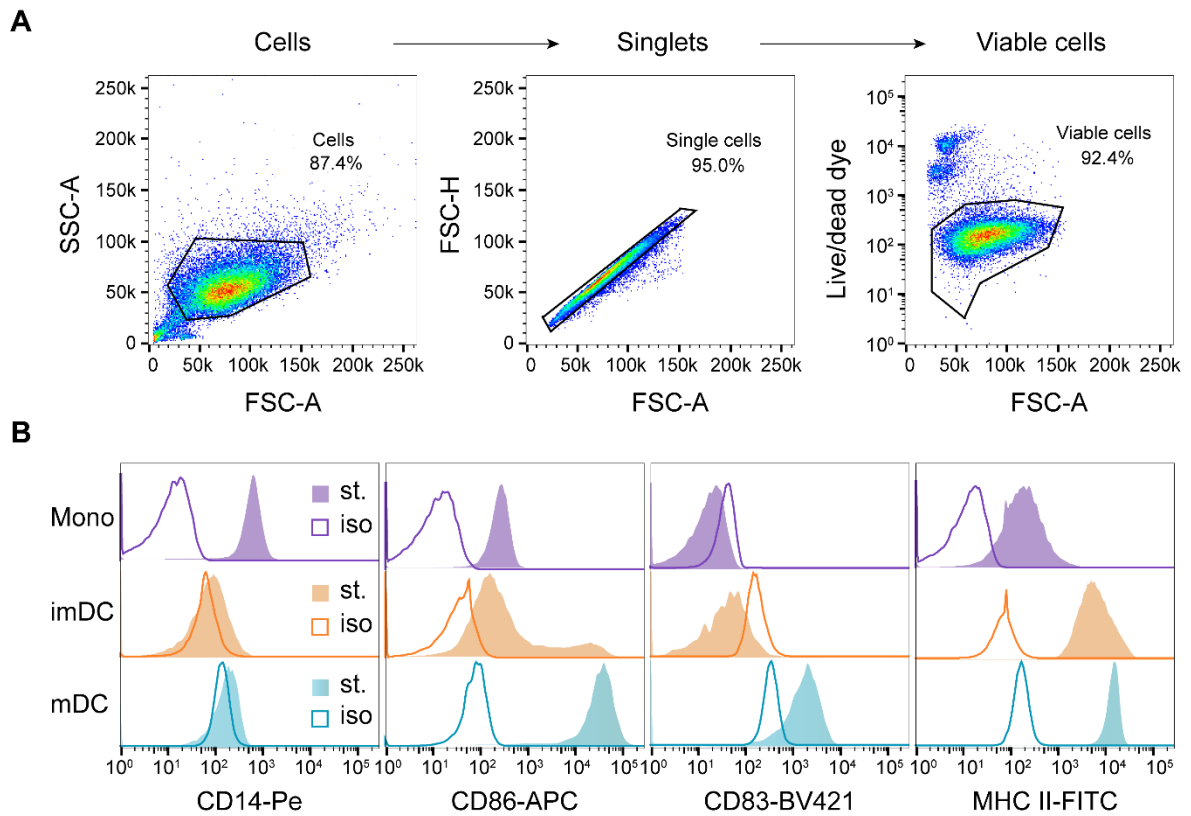
⁵Cluster of Excellence (EXC 2155) - Resolving Infection Susceptibility, Hannover Medical School,
Carl-Neuberg-Str. 1, 30625 Hannover, Germany

#contributed equally, *To whom correspondence may be addressed: tampe@em.uni-frankfurt.de

†current address: Mainz Biomed Germany GmbH, Robert-Koch-Str. 50, 55129, Germany

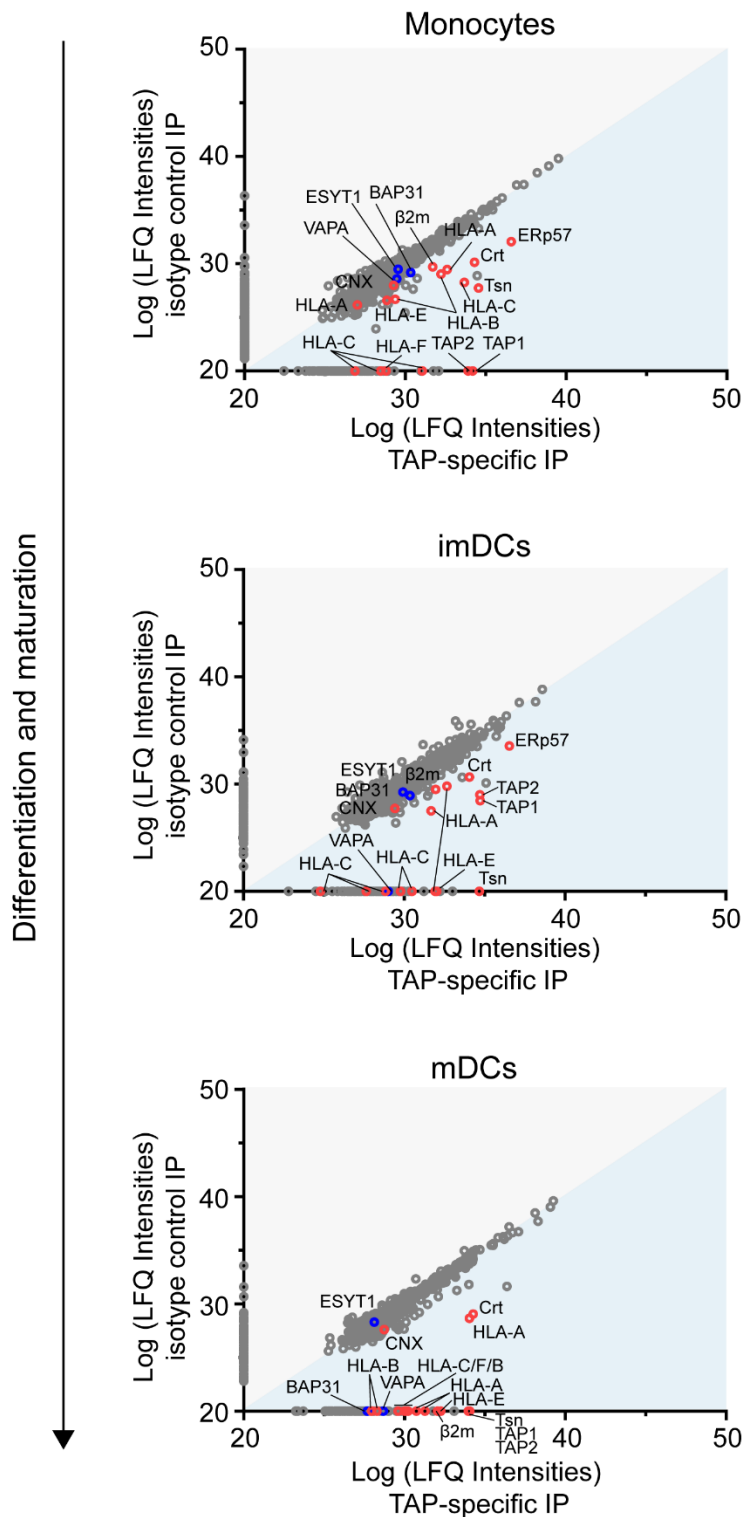
§current address: Division of Infectious Diseases and Geographic Medicine, Stanford Medicine,
Palo Alto, California 94305, USA

Supplementary Figures



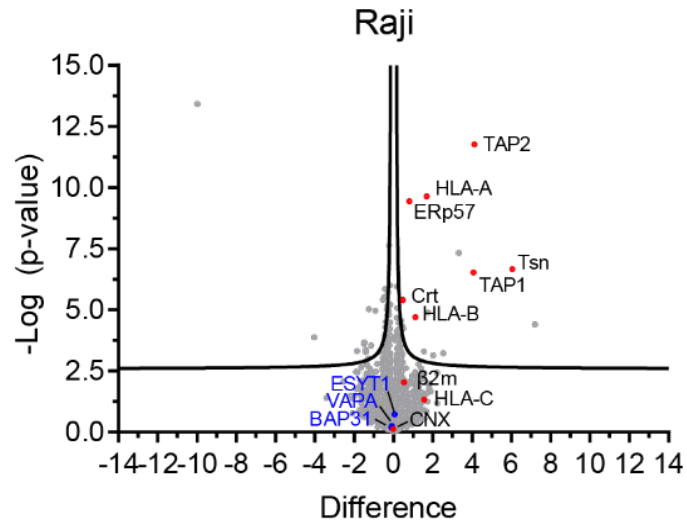
Supplementary Figure 1: Altered phenotypes during moDC differentiation.

A Gating strategy illustrating cell population subgating to singlets followed by viable cell discrimination. Percentage of parent population is annotated. Cells gated as viable were used for differentiation assessment. **B** Surface expression of activation markers CD14, CD86, CD83, and MHC II was analyzed in monocytes (Mono, magenta), imDCs (orange), and mDCs (teal) by flow cytometry (stained, st.). Isotype (iso) controls are shown in the corresponding color as a single line.



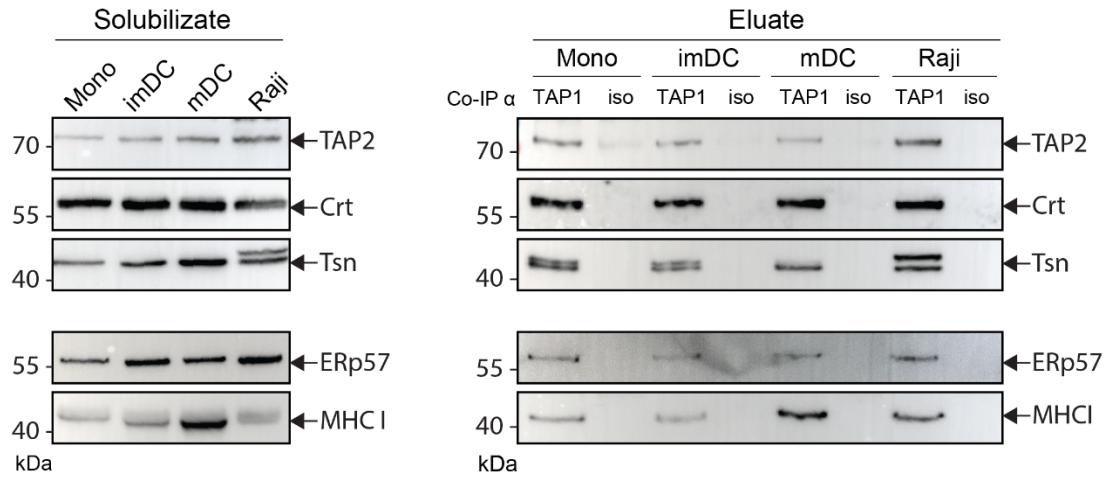
Supplementary Figure 2: TAP/PLC interactome in monocytes, imDC, and mDCs.

Monocytes were isolated from PBMCs and differentiated into imDCs and mDCs. Samples from each step of differentiation were analyzed by TAP1-specific co-IP and subsequent LC-MS/MS. Plots display the label-free quantitation (LFQ) intensities of identified proteins from TAP-specific and control IPs. Logarithmized LFQ intensities of Proteins below 20 have been set artificially to 20 to simplify the graphical presentation. Proteins known to be part of the PLC complex are shown in red and the three putative interacting proteins BAP31, VAPA, and ESYT1 are displayed in blue. Proteins within the light blue area are enriched during TAP1-specific immunoprecipitation.



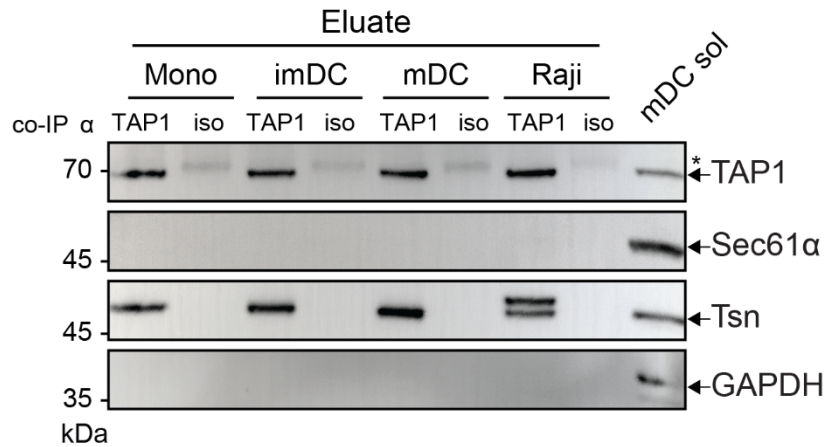
Supplementary Figure 3: TAP/PLC interactome in Raji cells.

Volcano plot displays difference and statistical significance of identified proteins of TAP-based co-IP from Raji cells. Plots were generated by PERSEUS software. Important proteins are highlighted in red and blue. False discovery rate: 0.05, S1: 0.04.



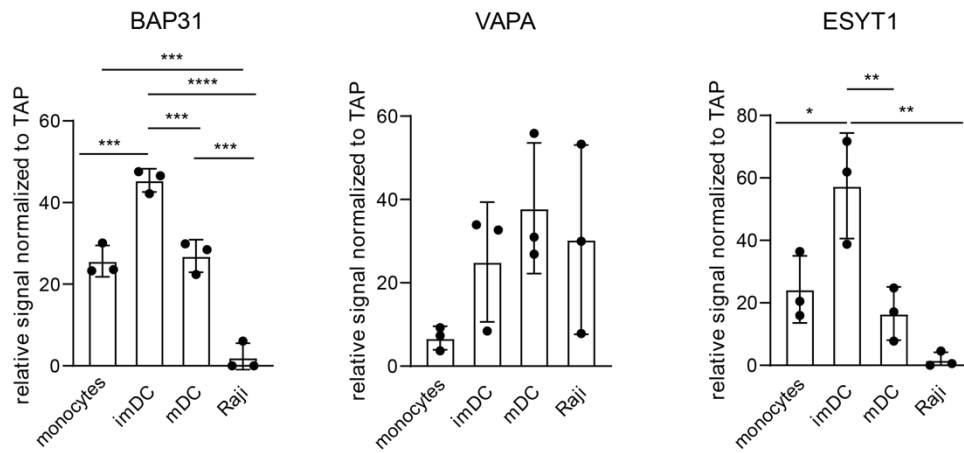
Supplementary Figure 4: Core PLC components in TAP1 co-immunoprecipitation.

Monocytes (mono), imDCs, mDCs, and Raji cells were solubilized in 1% (w/v) digitonin and TAP1 (mAb 148.3) co-immunoprecipitated. A corresponding isotype antibody (iso) was used as a control. Proteins were separated on SDS-PAGE and subsequently immunoblotted. To avoid donor dependencies, two to three donors were pooled for each primary cell type. Left panel shows cell lysate material after solubilization and ultracentrifugation (solubilizate). On the right panel, the eluate samples after co-immunoprecipitation are presented. Core components of the PLC, including TAP2, calreticulin (CRT), tapasin (Tsn), ERp57, and MHC I, are detected by immunoblotting using specific antibodies.



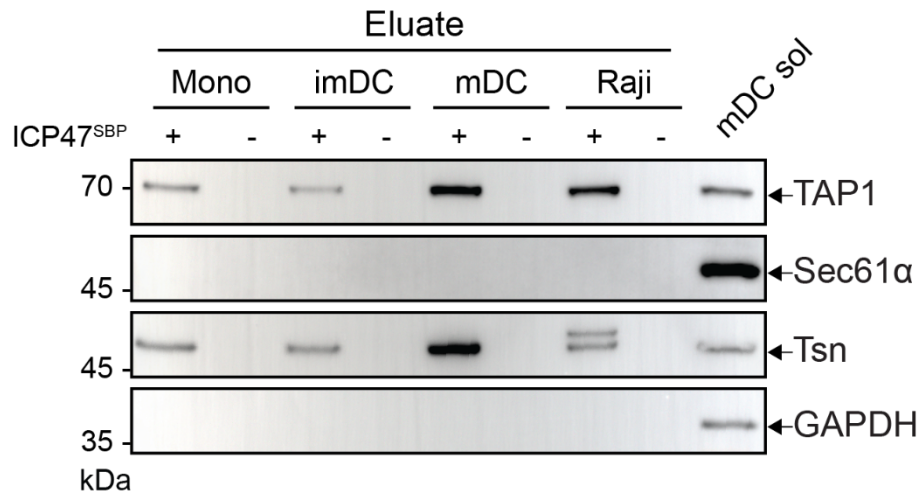
Supplementary Figure 5: Specific anti-TAP1 co-IP of PLC components.

Monocytes (mono), imDCs, mDCs, and Raji cells were solubilized in 1% (w/v) digitonin and TAP1 (mAb 148.3) co-immunoprecipitated. A corresponding isotype antibody (iso) was used as a control. Proteins were separated on SDS-PAGE and subsequently immunoblotted. To avoid donor dependencies, two to three donors were pooled for each primary cell type. Elution samples were loaded. As positive control, the solubilizate of mDCs was loaded on the last lane. Core components of the PLC, including TAP1 and tapasin (Tsn), were detected by immunoblotting in all TAP1 co-IP lanes and the solubilizate. Sec61 α , as ER-marker control, could only be detected in the solubilizate. Glycerinaldehyd-3-phosphat-Dehydrogenase (GAPDH) was used as control. * IgG from TAP1 and isotype antibodies.



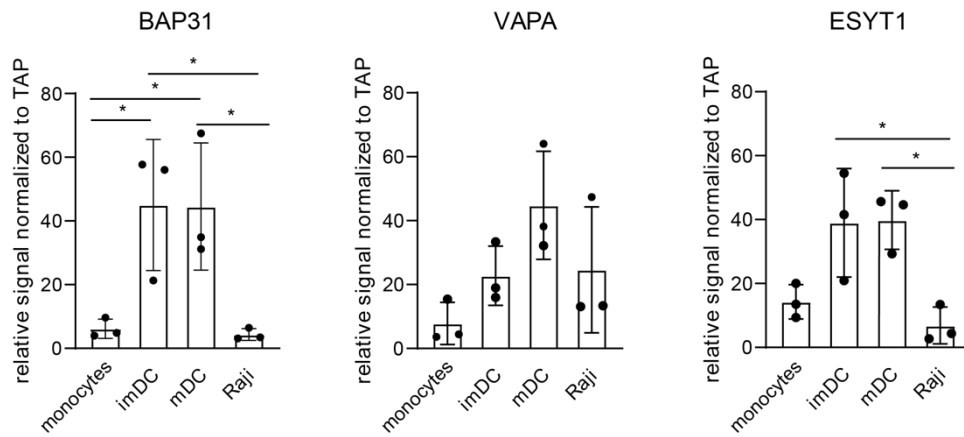
Supplementary Figure 6: Relative quantification of interaction partners after TAP1 co-IP.

Monocytes, imDCs, mDCs, and Raji cells were solubilized in 1% (w/v) digitonin and TAP1 co-immunoprecipitated using the monoclonal antibody mAb 148.3. In the immunoprecipitated fraction, BAP31, VAPA, and ESYT1 were quantified and normalized to TAP1 band intensity. Each symbol represents one independent experiment of cells pooled from at least three donors per cell type. One-way ANOVA with Tukey's post hoc was performed. *, $P \leq 0.05$; **, $P \leq 0.01$; ***, $P \leq 0.005$; ****, $P \leq 0.0001$.



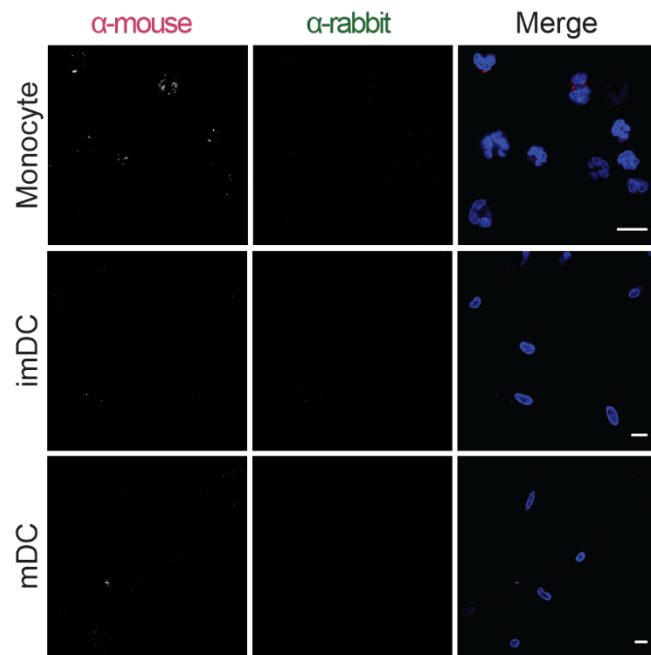
Supplementary Figure 7: Specific ICP47^{SBP} pull-down of PLC components.

Monocytes (mono), imDCs, mDCs, and Raji cells were solubilized in 1% (w/v) digitonin and ICP47^{SBP} was added to a half of every sample. Cells without addition of ICP47^{SBP} were used as a control. Proteins were separated on SDS-PAGE and subsequently immunoblotted. To avoid donor dependencies, two to three donors were pooled together for each primary cell type. Elution samples were loaded. As positive control, the solubilize of mDCs was loaded on the last lane. Core components of the PLC, including TAP1 and tapasin (Tsn), are detected by immunoblotting in all ICP47^{SBP} lanes and the solubilize. In addition, Sec61α, as ER-marker control, could only be detected in the solubilize. GAPDH was used as control.



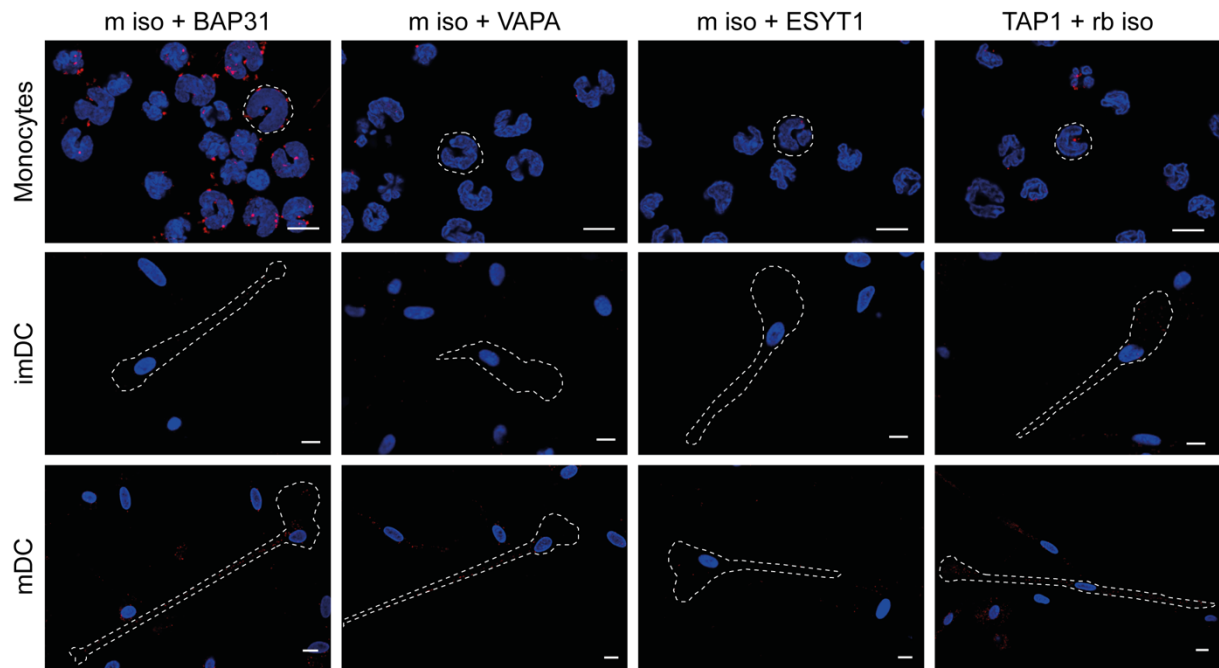
Supplementary Figure 8: Relative quantification of interaction partners after ICP47^{SBP} pull-down

Monocytes, imDCs, mDCs, and Raji cells were solubilized in 1% (w/v) digitonin, and components of the native PLC were affinity-purified using via ICP47^{SBP}. In the eluted PLC fraction, BAP31, VAPA, and ESYT1 were quantified and normalized to TAP1 band intensity. Each symbol represents one independent experiment of cells pooled from at least three donors per cell type. One-way ANOVA with Tukey's post hoc was performed. *, $P \leq 0.05$.



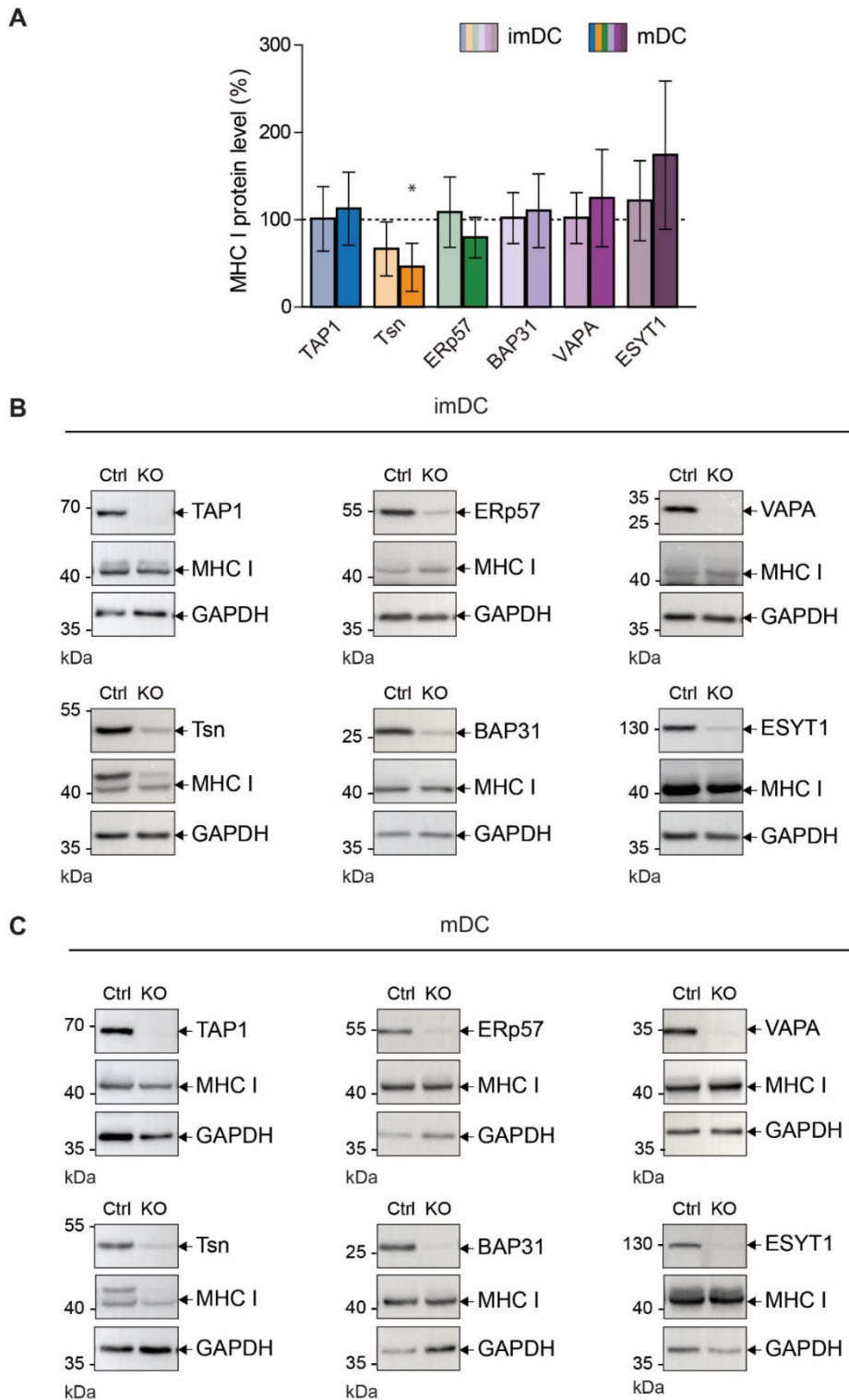
Supplementary Figure 9: moDCs labeling with secondary antibodies only.

To determine the unspecific binding of the anti-mouse AF647 and anti-rabbit AF532 secondary antibodies, monocytes, imDC and mDC were immunolabeled with secondary antibodies, in absence of primary antibodies and imaged in the same setting as Main Figure 3. Nuclei were stained with DAPI. Scale bar, 10 μ m.



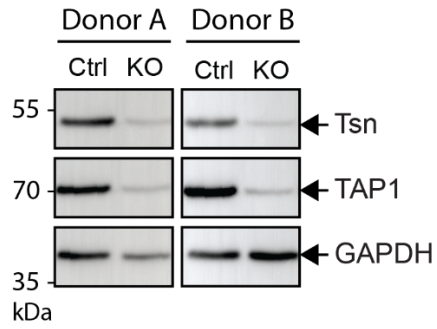
Supplementary Figure 10: Background staining of proximity ligation assay in moDCs.

To determine unspecific signals of the proximity ligation assay, monocytes, imDC, and mDC were immunolabeled with BAP31 + mouse isotype, VAPA + mouse isotype, ESYT1 + mouse isotype, and TAP1 + rabbit isotype, and measured in the same setting as Main Figure 4B. Scale bar, 10 μ m.



Supplementary Figure 11: Protein level after knockout in imDC and mDC.

Monocytes were subjected to CRISPR/Cas9 knockout and differentiated into imDC or mDC. **A** Normalized protein abundance of MHC I in single knockout moDC compared to control moDC (donors analyzed for imDC $n \geq 6$, and mDC $n \geq 5$). Mean \pm SD were plotted. Statistical analysis data was performed with t test with correction for multiple comparisons. *, $P \leq 0.01$. **B** imDC and **(C)** mDC detection of the knockout target proteins TAP1, tapasin (Tsn), ERp57, BAP31, VAPA and ESYT1 analyzed by immunoblot, as well as the relative abundance of MHC I. Control gRNA-nucleofected cells were used as comparison. GAPDH was used as loading control.



Supplementary Figure 12: TAP1 downregulation after tapasin knockout.

Monocytes were subjected to CRISPR/Cas9 knockout and differentiated into mDC. After knockout of tapasin (Tsn), the relative abundance of TAP1 in mDC was analyzed by immunoblotting. The results of two exemplary donors are shown. Control gRNA-nucleofected cells were used as comparison. GAPDH was used as loading control.

Supplementary Table 1: crRNA sequences for RNP formation. Sequences were selected from IDT or GenScript® databases.

crRNA	(5'--> 3')
TAP1 #1	CTTGTAGAATCCAGTCAGTG
TAP1 #2	GGTGGGCAGCTGGTGACCAG
TAP1 #3	AATCTGTACCAGCCCACCGG
Tsn #1	AACCAACACTCGATCACCGC
Tsn #2	CTTGTCCCAGTCTCACTCGA
Tsn #3	AAGGTCCCATTTCCGGTCCA
ERp57 #1	GTCCGTGAGTTCTAGCACGT
ERp57 #2	CTCCGACGTGCTAGAACTCA
VAPA #1	GTCATCCTTCGTGTGATAAC
VAPA #2	TGAAGACTACAGCACCTCGC
BAP31 #1	GAGTCACCAGGCGTCTAAGC
BAP31 #2	TGCCACCTTCCTCTATGCGG
BAP31 #3	TCGGAAGTATGATGATGTGA
ESYT1	CAGGACAACCAGGCACCGTG

Supplementary Table 2: Antibodies for flow cytometry.

Antibody	Clone	Cat.no, Company	Secondary antibody
FITC α -human-MHC II	Tü39	361706, Biolegend	--
FITC mouse IgG2a, κ isotype	MOPC-173	555573, BD	--
APC α -human-CD86	IT2.2	305411, Biolegend	--
APC mouse IgG2b, κ	MPC-11	400322, Biolegend	--
BV421 α -human-CD83	HB15e	305324, Biolegend	--
BV421 mouse IgG1, κ	MOPC-21	400157, Biolegend	--
PE α -human-CD14	M5E2	301806, Biolegend	--
PE Mouse IgG2a, κ	MOPC-173	400212, Biolegend	--
APC α -human-MHC I	W6/32	311410, Biolegend	--
APC mouse IgG2a, κ	MOPC-173	400220, Biolegend	--
APC α -human HLA-A2	REA517	130-116-657, Miltenyi	--
APC α -human HLA-A3	REA950	130-115-741, Miltenyi	--
PE-Vio 615 α -human HLA-A3	REA950	130-115-845, Miltenyi	--
APC human IgG1 isotype	QA16A12	403505, Biolegend	--
α -TAP1	148.3	Hybridoma, in-house	α -mouse AF488
α -BAP31	EPR3878(2)	ab109304, Abcam	α -rabbit AF488
α -VAPA	polyclonal	HPA009174, Sigma-Aldrich	α -rabbit AF488
α -ESYT1	polyclonal	HPA076926, Sigma-Aldrich	α -rabbit AF488